Virologica Sinica (2018) 33:335–344
https://doi.org/10.1007/s12250-018-0045-y

www.virosin.org
www.springer.com/12250

RESEARCH ARTICLE

Tandem 3′ UTR Patterns and Gene Expression Profiles of Marc-145 Cells During PRRSV Infection

Ying Wei[1] · Jie Li[1,2] · Yun Zhang[1] · Chunyi Xue[1] · Yongchang Cao[1]

Received: 11 May 2018 / Accepted: 4 July 2018 / Published online: 1 August 2018

Abstract

Porcine reproductive and respiratory syndrome virus (PRRSV) causes substantial economic losses to the global pig industry. Alternative polyadenylation (APA) is a mechanism that diversifies gene expression, which is important for tumorigenesis, development, and cell differentiation. However, it is unclear whether APA plays a role in the course of PRRSV infection. To address this issue, in this study we carried out a whole-genome transcriptome analysis of PRRSV-infected Marc-145 African green monkey kidney cells and identified 185 APA switching genes and 393 differentially expressed genes (DEGs). Most of these genes were involved in cellular process, metabolism, and biological regulation, and there was some overlap between the two gene sets. DEGs were found to be more directly involved in the antiviral response than APA genes. These findings provide insight into the dynamics of host gene regulation during PRRSV infection and a basis for elucidating the pathogenesis of PRRSV.

Keywords Porcine reproductive and respiratory syndrome virus (PRRSV) · Alternative polyadenylation (APA) · Differentially expressed genes (DEGs) · Whole-genome transcriptome analysis

Introduction

Porcine reproductive and respiratory syndrome (PRRS), also known as blue ear disease, is one of the most important porcine infectious diseases affecting the global pig industry. PRRS is characterized by symptoms in infected pregnant sows including anaphase abortion, stillbirth, mummified or weak fetus, respiratory distress (interstitial pneumonia), and high morality of pigs at various ages, especially piglets (Hopper *et al.* 1992). The disease was first reported in the United States in 1987 and is now widely transmitted in many swine-producing countries (Collins *et al.* 1992). The causative agent of the disease, PRRS virus (PRRSV), is an enveloped, positive-sense, single-stranded RNA virus belonging to the order *Nidovirales*, family *Arteriviridae* (Cavanagh 1997). The viral genome is approximately 15 kb with a 5′ cap, 3′ polyadenylation (poly[A]) sequence, and at least 11 overlapping open reading frames (Kappes and Faaberg 2015). PRRSV is classified into two genotypes: European type 1 (prototype Lelystad-LV) and American type 2 (prototype VR2332) (Allende *et al.* 1999).

PRRSV causes persistent infection with a long period of viremia, macrophage tropism, and antibody-dependent enhancement (Butler *et al.* 2014; Cancel-Tirado *et al.* 2004). Vaccination is typically used to prevent and control the disease (Chia *et al.* 2010). However, constant mutations in the PRRSV genome lead to antigen shift and drift, making traditional inactivated and attenuated vaccines ineffective. Identifying host factors that enable PRRSV infection may provide new approaches to disease prevention.

Different mRNA variants of genes are produced through selective transcription initiation, splicing, and poly(A). The protein isoforms thus generated play an important role in the precise spatial and temporal control of gene expression networks. Alternative poly(A) (APA) is a regulatory mechanism for generating mRNAs with distinct 3′ untranslated regions (3′ UTRs) or code sequences of

Ying Wei and Jie Li have contributed equally to this work.

✉ Yongchang Cao
caoych@mail.sysu.edu.cn

[1] State Key Laboratory of Biocontrol, School of Life Sciences, Sun Yat-sen University, Guangzhou 510006, China

[2] School of Biology and Food Engineering, Changshu Institute of Technology, Changshu 215500, China

distinct isoforms via recognition of different poly(A) signals (PAS). 3′ UTRs of varying length containing diverse *cis*-regulatory elements including microRNA- and RNA binding protein-binding sites thus influence mRNA stability, transport, and translation efficiency (Fabian *et al.* 2010; Elkon *et al.* 2013; Tian and Manley 2013). APA sites are present in over half of human genes and are also abundant in mouse and other model animals (Shi 2012; Sun *et al.* 2012). There is increasing evidence suggesting that APA is a mechanism for diversifying gene expression in tumorigenesis, development, and cell differentiation (Sandberg *et al.* 2008; Fu *et al.* 2011; Hilgers *et al.* 2011).

With the development of 3′ end sequencing technology, research has focused on the switching of APA sites during viral infection and the search for novel infection biomarkers. In this study, we used the sequencing alternative poly(A) sites (SAPAS) method combined with *in vitro* transcription (IVT) to profile APA sites switching events and differentially expressed genes (DEGs) in PRRSV-infected Marc-145 cells in order to clarify the dynamics of host–pathogen interactions. We identified 185 APA sites switching genes and 393 DEGs in infected Marc-145 African green monkey kidney cells, and found that these two gene sets reflect distinct but complementary mechanisms in the host response to PRRSV infection.

Materials and Methods

Cell Culture and PRRSV Infection

Marc-145 cells were cultured in Dulbecco's Modified Eagle's Medium (Gibco, Grand Island, NY, USA) supplemented with 10% fetal bovine serum (Gibco) in an incubator at 37 °C and 5% CO_2. PRRSV was provided by Professor Yaosheng Chen (Sun Yat-sen University, Guangzhou China) and were prepared in Marc-145 cells. The cells were infected at a multiplicity of infection of 5, with mock-infected cells serving as a control. Cells were collected at 0, 6, 12, 24, and 36 h post-infection (hpi). A total of nine samples were used for library preparation.

IVT-SAPAS Library Preparation and Sequencing

Sequencing libraries were prepared as previously described (Fu *et al.* 2015). Briefly, total RNA was extracted from Marc-145 cells using TRIzol reagent (Invitrogen, Carlsbad, CA, USA). Approximately 2 μg total RNA were fragmented by heating, and specific primers were used for reverse transcription and PCR amplification. Fragments 250–400 bp in size were excised and purified with Agencourt Ampure magnetic beads (Beckman Coulter, Brea, CA, USA). The average size was determined with a Model 2100 bioanalyzer (Agilent Technologies, Santa Clara, CA, USA). The final pooled fragments were sequenced from the 3′ end with Genome Analyzer IIx (Illumina, San Diego, CA, USA).

Profiling of APA Sites and DEGs

Sequencing was performed as previously described (Fu *et al.* 2011). Briefly, raw reads were filtered and trimmed for quality control utilizing a Perl script and then mapped to the *Chlorocebus sabaeus* genome. The genomic location of poly(A) sites were defined based on gene annotations. The poly(A) signal of each site was selected based on its genomic sequences. Genes with significant P values corresponding to a false discovery rate < 0.05 and fold change > 1.5 were identified as significant DEGs. A combined model to test tandem APA switching events was generated (Fu *et al.* 2011) by identifying genes with significant APA switching between infected and normal cells with the linear trend and independence tests. Gene Ontology (biological process) analysis was performed with PANTHER (http://www.pantherdb.org/). Kyoto Encyclopedia of Genes and Genomes (KEGG) pathway analysis was performed using Database for Annotation, Visualization, and Integrated Discovery (https://david.ncifcrf.gov/).

Quantitative Real-Time (qRT)-PCR Validation

Poly(A) sites were divided into two supersites (proximal and distal). Primers were designed to target the upstream region of the two supersites based on published sequences. cDNA was synthesized from total RNA using the PrimeScript RT reagent kit (Takara Bio, Otsu, Japan), and qRT-PCR was performed on a LightCycler 480 real-time PCR system (Roche Diagnostics, Indianapolis, IN, USA) using the SYBR Pre-mix ExTaq II kit (Takara Bio) in a 10 μL reaction volume. Each cDNA was analyzed in triplicate. A similar process was used to analyze DEGs.

Raw Data Availability

Raw poly(A)-sequencing data are available from https://figshare.com/s/d17f00575d6d4c3c662e.

Results

Poly(A) Site Profiling in Marc-145 Cells

To investigate the dynamics of host–pathogen interactions based on poly(A) pattern and gene expression profile

during PRRSV infection, we used the SAPAS method combined with IVT to generate nine IVT-SAPAS libraries (C0, C6, T6, C12, T12, C24, T24, C36, and T36, where C and T denote control and treatment groups, respectively, and numbers indicate hpi).

A total of 332 million raw reads were generated by Illumina sequencing. After mapping to the monkey genome and internal priming filtering, about 156 million reads were obtained for poly(A) sites analysis (Table 1). Only 39% of reads used University of California at Santa Cruz annotated poly(A) sites, indicating that IVT-SAPAS was effective in detecting novel poly(A) sites, especially in samples with low mRNA expression levels (Fig. 1A). Additionally, 22% and 12% of reads were located in the intergenic region and 1 kb downstream of the gene's 3′ UTR. About 2×10^5 variable poly(A) sites—only 13% (Fig. 1B) of which are known—accounted for 58% of reads (Fig. 1A).

We arranged the annotated 3′ UTR APA sites in tandem based on the stop codon and combined these with poly(A) site profiling as previously described (Fu *et al.* 2011), and found that 6536 genes had tandem 3′ UTRs, while 34.33% had at least two tandem 3′ UTR poly(A) sites (Fig. 1C). Poly(A) sites switching may regulate a variety of biological functions. The average distribution of distances between poly(A) site and stop codon was 426 bp (median: 270 bp). Median distances between the stop codon and proximal and distal poly(A) sites were 237 and 720 bp, respectively (Fig. 1D). These results reveal the detailed landscape of poly(A) site usage in Marc-145 cells and suggest an important regulatory role for APA in the monkey genome.

Signaling via Poly(A) Sites in Marc-145 Cells

The poly(A) signal (PAS) is an important *cis*-acting element in 3′ end processing that is located 10–30 nt upstream of the cleavage site. The six-nucleotide base sequence is recognized by cleavage poly(A) specificity factor (Elkon *et al.* 2013). To date, 12 types of PAS have been identified, with AATAAA and ATTAAA being the most common (Proudfoot 2011), which was confirmed by our finding that the usage frequency was close to 50%. Our data suggest that poly(A) is dynamic; moreover, 26.6% of the six PAS dimers were not observed (Fig. 2), suggesting that there are other regulatory mechanisms.

Tandem 3′ UTR Switching and Regulation of Gene Expression in PRRSV-Infected Marc-145 Cells

The IVT-SAPAS method can be used not only to analyze APA, but also to quantify the expression of a gene based on an analysis of the 3′ UTR of its transcripts (Jia *et al.* 2017). Genes with tandem 3′ UTR lengths that differed significantly between libraries were defined as APA switching genes. We identified 19, 17, 52, and 142 such genes at 6, 12, 24, and 36 hpi, respectively (Fig. 3A). In total, there were 185 APA switching genes (false discovery rate [FDR] < 0.05, Rcut ≤ 0.05) after PRRSV infection, of which 141

Table 1 Summary of IVT-SAPAS data from Illumina sequencing.

	C0	C6	T6	C12	T12	C24	T24	C36	T36
Raw reads	36,116,763	37,833,985	39,850,440	38,288,537	37,213,155	35,254,213	35,489,443	32,531,227	39,643,333
Qualified reads	36,013,570	37,721,051	39,746,102	38,110,460	37,107,821	35,184,082	35,392,059	32,436,994	39,571,134
Mapped to genome	27,228,751	29,621,971	29,860,943	29,509,068	27,992,912	27,078,891	26,201,743	25,142,986	27,321,962
Uniquely mapped to genome	18,427,920	19,813,985	20,002,551	20,185,258	18,965,744	18,450,107	18,187,357	17,609,767	19,445,450
Mapped to nuclear genome	18,138,375	19,429,398	19,617,915	19,827,454	18,579,277	17,859,723	17,816,024	17,216,172	19,064,918
After IP* filter	16,152,340	17,568,103	17,525,620	17,621,090	16,646,621	15,955,533	15,846,326	15,195,222	16,840,141
Genes sampled by reads	13,239	13,115	13,246	13,228	13,189	13,292	13,275	13,276	13,126
Cleavage clusters	119,432	113,629	122,983	119,304	113,554	109,885	114,604	112,814	111,551
Known poly A sites sampled	7499	7432	7524	7495	7418	7490	7561	7450	7558
Putative novel poly A sites	111,933	106,197	115,459	111,809	106,136	102,395	107,043	105,364	103,993
Genes sampled by cleavage clusters	12,037	12,052	12,166	12,110	12,081	12,156	12,170	12,131	12,084

*IP internal priming.

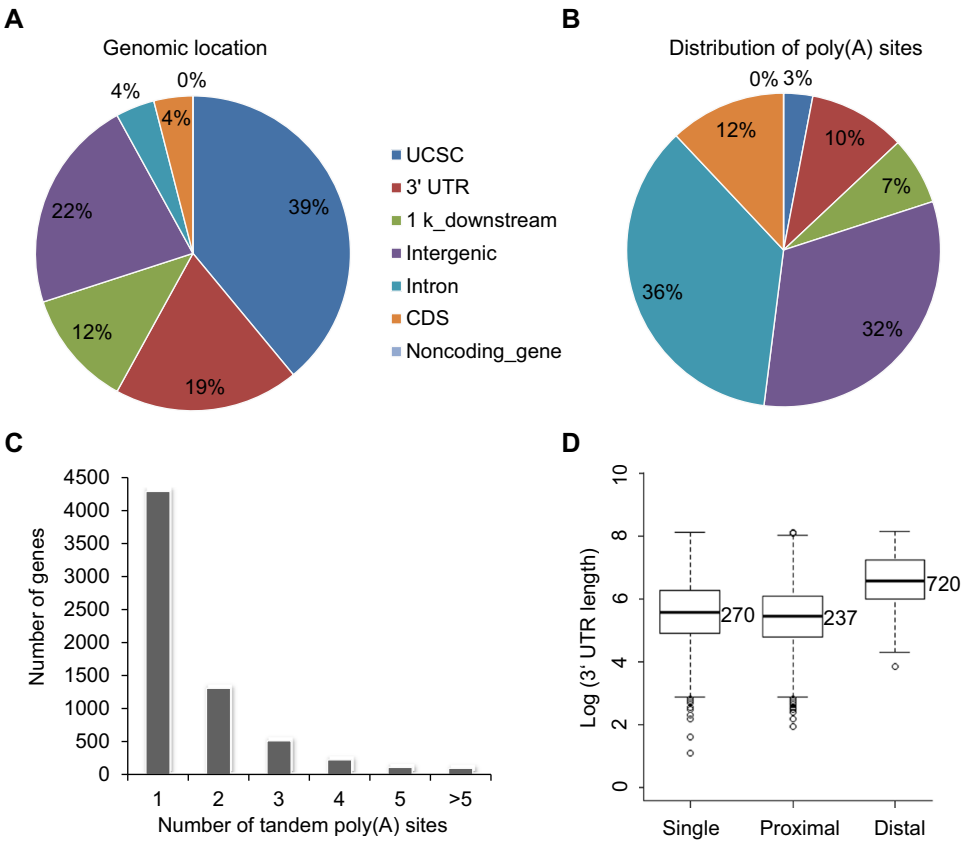

Fig. 1 Sequencing reads and poly(A) sites in Marc-145 cells. **A** Genomic location of sequencing reads. **B** Distribution of poly(A) sites in the genome. **C** Genes with different numbers of tandem poly(A) sites. **D** Histogram of the median distance between stop codon and poly(A) sites in genes with single poly(A) sites, and distance between stop codon and closest or longest poly(A) sites in genes with multiple poly(A) sites.

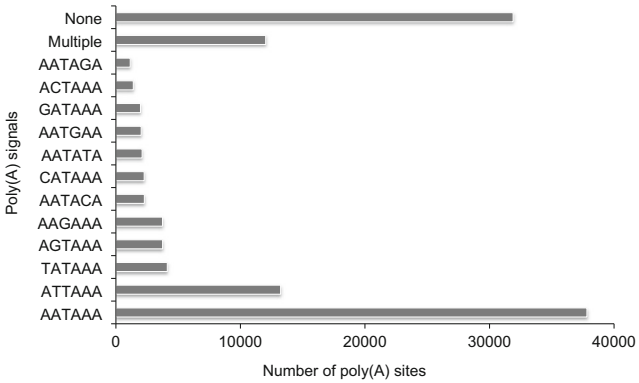

Fig. 2 Signaling via poly(A) sites in Marc-145 cells.

used shorter 3′ UTRs, 32 used longer 3′ UTRs, and 12 were dynamically regulated at different time points (Fig. 3B). Genes exhibiting a greater than 1.5-fold difference in expression and had an FDR < 0.05 were considered as differentially expressed. We identified 15, 14, 71 and 361 DEGs at 6, 12, 24, and 36 hpi, respectively (Fig. 3C). In total, there were 393 genes that were differentially regulated between mock- and PRRSV-infected samples, of which 234 were upregulated, 152 were downregulated, and 7 were dynamically regulated at different time points (Fig. 3B).

To clarify the functional relationship between APA sites and differential gene expression in antiviral immunity, we compared APA genes and DEGs and identified 35 genes involved in the simultaneous regulation of the two mechanisms, indicating that the two mechanisms are independent (Fig. 3D). Furthermore, a classification of gene function revealed that there was little difference in gene function between the two gene sets, which covered cellular and metabolic processes, biological regulation, and response to stimulus, among other categories (Fig. 3E, 3F). These results indicate that these two mechanisms are actively involved in the response to viral infection.

Dynamic Gene Regulation in PRRSV-Infected Marc-145 Cells

To clarify the changes in gene expression over the course of viral infection, we generated a growth curve. Viral titer increased slightly within 12 hpi and then rapidly thereafter (black curves, left Y axis; red curve, right Y axis) unlike mock-infected cells (blue curve, right Y axis), which is consistent with the sequencing data (Fig. 4A). We then analyzed the number of APA genes (Fig. 4B) and DEGs (Fig. 4C) at two sequential time points and found that their total numbers increased during the infection cycle, especially at 12–24 and 24–36 hpi, respectively, when viral

A

	6 h	12 h	24 h	36 h
Long	13	10	11	17
Short	6	7	41	125
Total	19	17	52	142

($P < 0.05$, FDR = 5%, Rcut ≤ 0.05)

B

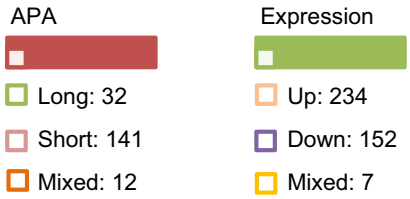

C

	6 h	12 h	24 h	36 h
Up	7	8	58	143
Down	8	6	13	218
Total	15	14	71	361

($P < 0.05$, FDR = 5%, Fold change > 1.5)

D

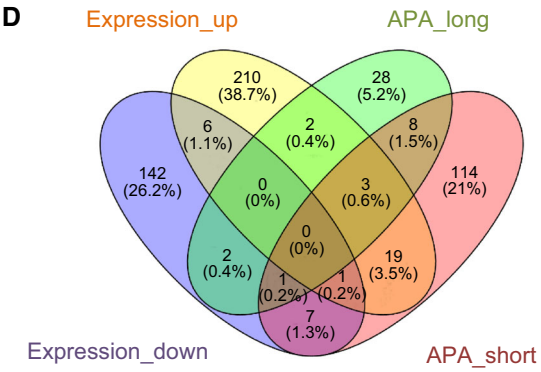

E

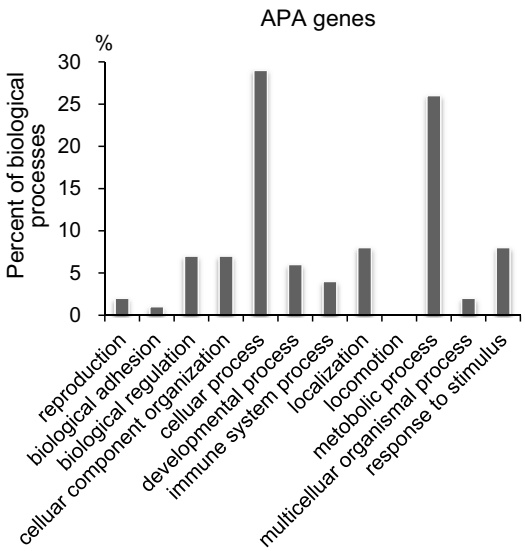

F

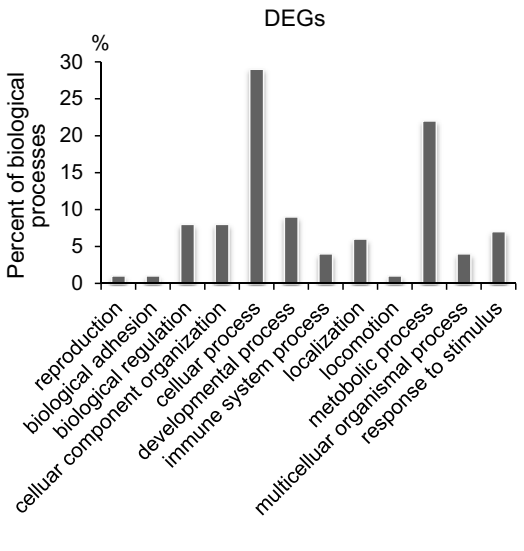

Fig. 3 Analysis of tandem 3′ UTR switching and regulation of gene expression in PRRSV-infected Marc-145 cells. **A** Summary of APA genes between samples at different time points. **B** Summary of APA genes and DEGs. **C** Summary of DEGs between samples at different time points. **D** Wayne chart of APA genes and DEGs. **E**, **F** Functional classification of APA genes (**E**) and DEGs (**F**).

replication was in the logarithmic phase, suggesting a robust antiviral response. It is possible that this was due to the induction of host interferon (IFN)-stimulated gene expression after viral infection.

The KEGG analysis ($P \leq 0.05$) showed that APA genes (Fig. 4D) and DEGs (Fig. 4E) were upregulated during the immune response to PRRSV infection. The DEGs were also associated with the adaptive immune response, including B and T cell receptor signaling pathways. Additionally, DEGs were more directly involved in the antiviral innate immune response than APA genes, including apoptosis and activation of IFN-stimulated pathways. These results suggest that the two mechanisms act cooperatively in the host response to PRRSV infection.

Summary and Validation of Mixed APA Genes and DEGs

To investigate the relationship between APA and DEGs, we identified genes common to the two gene sets at 36 hpi

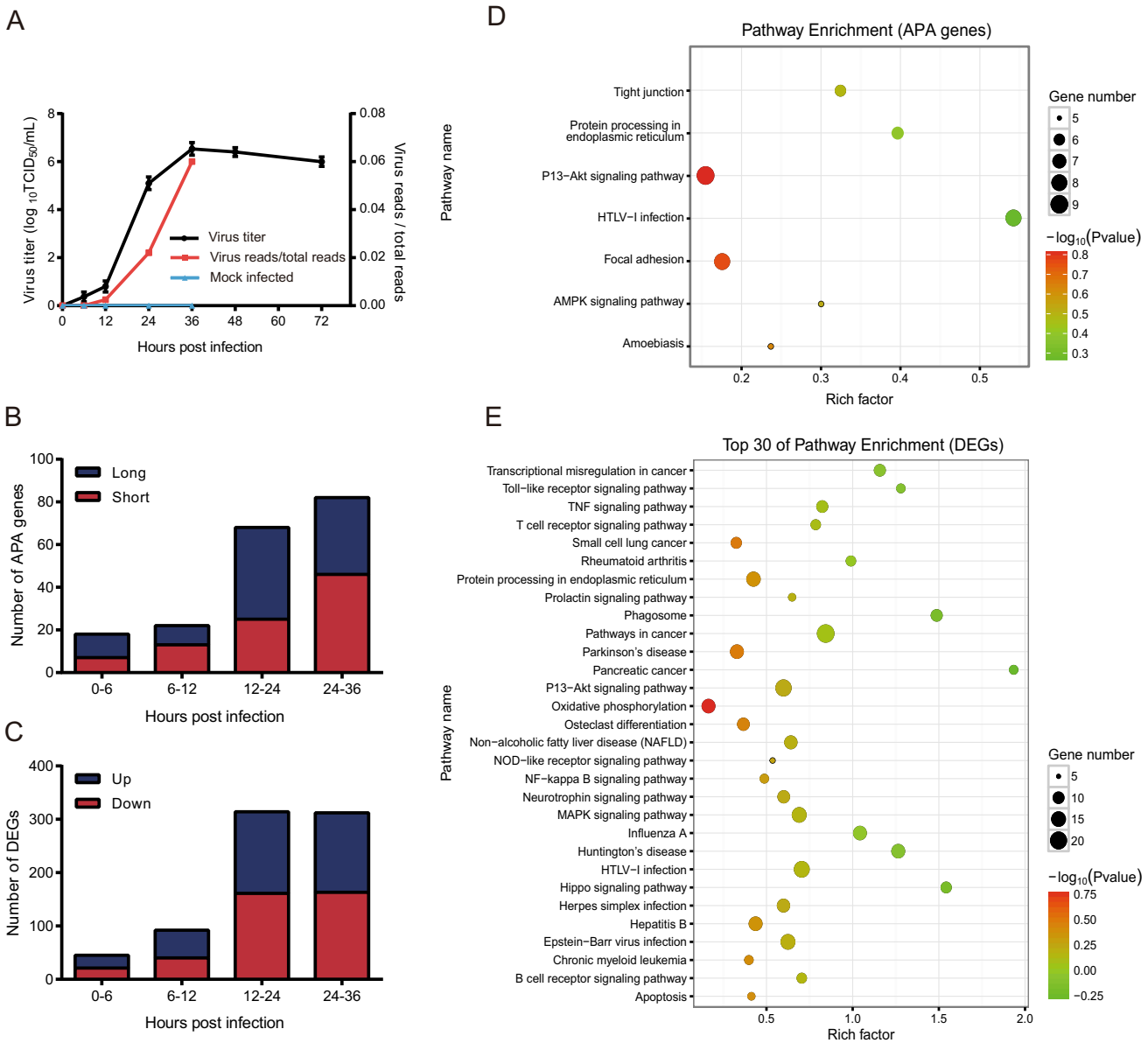

Fig. 4 Dynamic regulation in PRRSV-infected Marc-145 cells. **A** PRRSV growth curve and number of reads. **B**, **C** Regulation of APA genes (**B**) and DEGs (**C**) at two sequential time points. **D**, **E** KEGG analysis of APA genes (**D**) and DEGs (**E**).

(Table 2). Compared to the negative control group, infected cells preferentially utilized shorter 3′ UTRs. Accordingly, most genes involved in APA shortening were upregulated. Proteins associated with innate immunity including *JUN* and *NFKB1* were at the center of the protein interaction map and did not show interactions with other proteins (Fig. 5A). Six mixed APA genes (black columns in Fig. 5B) and DEGs (white columns in Fig. 5B) were validated by qRT-PCR and the results were consistent with the sequencing data.

Discussion

APA can affect the stability, transport, translation efficiency and subcellular location of mRNA by producing mRNA isomers with different 3′ UTRs (Fabian *et al.* 2010; Elkon *et al.* 2013; Tian and Manley 2013). During the differentiation of mouse B cells, the APA site in the IgM gene was altered, resulting in the conversion of IgM protein from a membrane-bound to a secretory type (Takagaki *et al.* 1996). Since this initial report (Danckwardt *et al.* 2011), APA sites have been reported in thousands of genes in yeast, zebrafish, mouse, and human, most of which cannot be detected by microarray analysis (Tian *et al.*

Table 2 Summary of mixed APA genes and DEGs at 36 hpi.

Gene symbol	Description	APA	Expression	PAS* (No.)
VPS4A	Vacuolar protein sorting 4 homolog A	Short	Up	2
BRD2	Bromodomain containing 2	Short	Up	2
E2F1	E2F transcription factor 1	Long	Up	2
FDFT1	Farnesyl-diphosphate farnesyltransferase 1	Short	Down	3
Rai14	Retinoic acid induced 14	Short	Up	3
AP3B1	Adaptor related protein complex 3 beta 1 subunit	Short	Up	3
Nfkb1	Nuclear factor kappa B subunit 1	Short	Up	3
Polr3d	RNA polymerase III subunit D	Short	Up	3
BAG3	BCL2 associated athanogene 3	Short	Up	3
Fbrsl1	Fibrosin-like 1	Short	Up	3
Phf12	PHD finger protein 12	Short	Up	3
JUN	Jun proto-oncogene, AP-1 transcription factor subunit	Long	Up	3
GLRX5	Glutaredoxin 5	Short	Down	4
NEDD9	Neural precursor cell expressed, developmentally down-regulated 9	Short	Up	4
POFUT1	Protein O-fucosyltransferase 1	Short	Up	4
CYR61	Cysteine rich angiogenic inducer 61	Short	Up	4
RHOB	Ras homolog family member B	Short	Up	4
Dnajb1	DnaJ heat shock protein family (Hsp40) member B1	Short	Up	4
ZFAND5	Zinc finger AN1-type containing 5	Short	Up	5
USP36	Ubiquitin specific peptidase 36	Short	Up	5
PIM1	Pim-1 proto-oncogene, serine/threonine kinase	Long	Up	5
FLNB	Filamin B	Short	Up	5
COL11A1	Collagen type XI alpha 1 chain	Short	Down	6
AZIN1	Antizyme inhibitor 1	Short	Up	7

*PAS, the poly(A) signal

2005; Ulitsky *et al.* 2012; Schlackow *et al.* 2013). Recent studies of PRRSV infection have focused on single antiviral immunomodulatory genes and changes in host gene expression at the whole-genome level (Ke *et al.* 2017; Li *et al.* 2017; Proll *et al.* 2017); however, there have been no reports of APA during PRRSV infection.

PRRSV is mainly propagated in porcine alveolar macrophages (Rossow *et al.* 1995). At present, there are no suitable porcine cell lines for *in vitro* PRRSV infection experiments, and Marc-145 cells are used instead since the virus can replicate and cause cytopathic changes in these cells (Zhao *et al.* 2016; Ji *et al.* 2017; Ma *et al.* 2018). In this study, we used Marc-145 cells for high-throughput transcriptome profiling of APA and changes in host gene expression during PRRSV infection by SAPAS combined with IVT.

APA is an important post-transcriptional mechanism for gene regulation. It was previously reported that 3′ UTRs tend to shorten during cell proliferation in early embryonic development and tumor transformation (Mayr and Bartel 2009; Hoque *et al.* 2013). Shorter 3′ UTRs have also been detected during T cell activation (Sandberg *et al.* 2008). On the contrary, the 3′ UTR was lengthened during embryonic development in mice (Ji *et al.* 2009). However, genome-wide poly(A) site switching and a gradual reduction in 3′ UTR length was associated with the response to vesicular stomatitis virus (VSV) infection in macrophages (Jia *et al.* 2017). In our study, more genes had shorter as compared to longer 3′ UTRs during the antiviral response to PRRSV infection. Given that this response requires the generation of large amounts of protein, 3′ UTR shortening may simplify gene regulation and thereby accelerate protein synthesis to improve the body's antiviral response.

It was recently that there was no clear correlation between tandem 3′ UTRs and mRNA abundance in the response to VSV infection in macrophages (Jia *et al.* 2017), which is consistent with our findings. During infection by Marek's disease virus, only 42 genes were simultaneously regulated by the two mechanisms (Li *et al.* 2017), which is close to the value observed here (35 genes). Our functional analysis showed that both APA genes and DEGs regulated variety of biological processes associated with the antiviral immune response, with the host not only modulating mRNA abundance but also switching poly(A) sites to

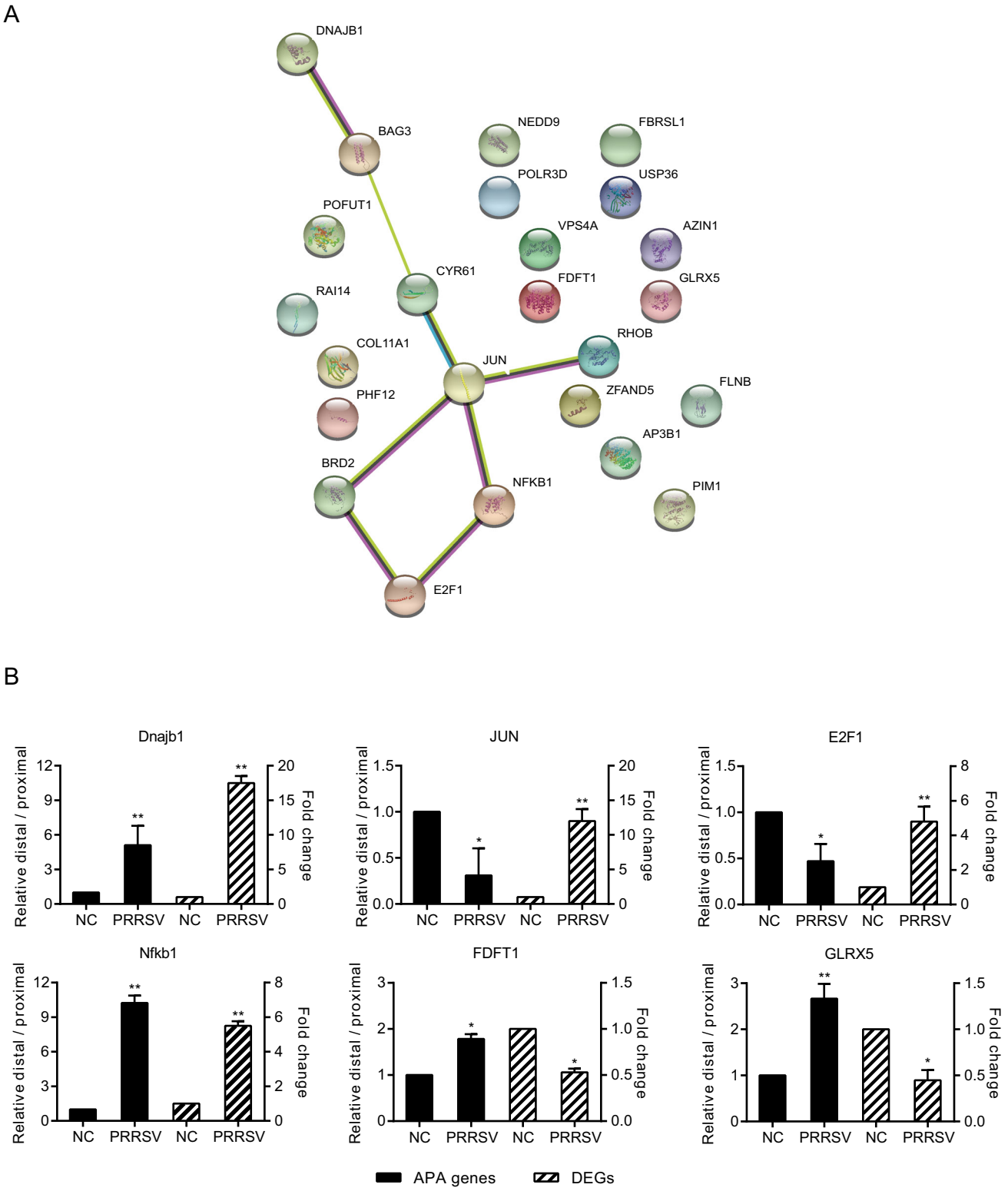

Fig. 5 Validation of mixed APA genes and DEGs. Protein interaction diagram (**A**) and qRT-PCR validation (**B**) of mixed APA genes and DEGs.

combat virus invasion. The KEGG pathway analysis showed that DEGs were enriched in antiviral immune response-related pathways to a greater extent than APA genes. This may be because regulation of APA is a relatively slow process. Further analysis of mixed APA genes and DEGs revealed that most upregulated genes showed

shortening of the APA sequence, although the mechanistic basis for this effect requires further investigation.

In conclusion, the results of our study reveal tandem 3′ UTR patterns in Marc-145 cells during PRRSV infection. Our data suggest that APA alters mRNA abundance, which may be correlated with the antiviral response. These findings highlight the functional relationship between APA and gene expression during PRRSV infection and provide a set of genes that are potential therapeutic targets for the prevention or treatment of PRRS.

Acknowledgements This work was supported by the Natural Science Foundation of Guangdong Province (2014A030312011) and Guangzhou Science and Technology Plan (201804020039).

Author Contributions YC, YW, JL and CX designed the study; YW performed the experiments; JL and YW analyzed the data; YW prepared the figures and tables; YW and YZ wrote the main manuscript. YC checked and finalized the manuscript. All authors read and approved the final manuscript.

Compliance with Ethical Standards

Conflict of interest The authors declare that they have no conflict of interest.

Animal and Human Rights Statement This article does not contain any studies with human or animal subjects performed by any of the authors.

References

Allende R, Lewis TL, Lu Z, Rock DL, Kutish GF, Ali A, Doster AR, Osorio FA (1999) North American and European porcine reproductive and respiratory syndrome viruses differ in non-structural protein coding regions. J Gen Virol 80:307–315

Butler JE, Lager KM, Golde W, Faaberg KS, Sinkora M, Loving C, Zhang YI (2014) Porcine reproductive and respiratory syndrome (PRRS): an immune dysregulatory pandemic. Immunol Res 59:81–108

Cancel-Tirado SM, Evans RB, Yoon KJ (2004) Monoclonal antibody analysis of porcine reproductive and respiratory syndrome virus epitopes associated with antibody-dependent enhancement and neutralization of virus infection. Vet Immunol Immunopathol 102:249–262

Cavanagh D (1997) Nidovirales: a new order comprising Coronaviridae and Arteriviridae. Arch Virol 142:629–633

Chia MY, Hsiao SH, Chan HT, Do YY, Huang PL, Chang HW, Tsai YC, Lin CM, Pang VF, Jeng CR (2010) The immunogenicity of DNA constructs co-expressing GP5 and M proteins of porcine reproductive and respiratory syndrome virus conjugated by GPGP linker in pigs. Vet Microbiol 146:189–199

Collins JE, Benfield DA, Christianson WT, Harris L, Hennings JC, Shaw DP, Goyal SM, McCullough S, Morrison RB, Joo HS, Et A (1992) Isolation of swine infertility and respiratory syndrome virus (isolate ATCC VR-2332) in North America and experimental reproduction of the disease in gnotobiotic pigs. J Vet Diagn Investig 4:117–126

Danckwardt S, Gantzert AS, Macher-Goeppinger S, Probst HC, Gentzel M, Wilm M, Grone HJ, Schirmacher P, Hentze MW, Kulozik AE (2011) p38 MAPK controls prothrombin expression by regulated RNA 3′ end processing. Mol Cell 41:298–310

Elkon R, Ugalde AP, Agami R (2013) Alternative cleavage and polyadenylation: extent, regulation and function. Nat Rev Genet 14:496–506

Fabian MR, Sonenberg N, Filipowicz W (2010) Regulation of mRNA translation and stability by microRNAs. Annu Rev Biochem 79:351–379

Fu Y, Sun Y, Li Y, Li J, Rao X, Chen C, Xu A (2011) Differential genome-wide profiling of tandem 3′ UTRs among human breast cancer and normal cells by high-throughput sequencing. Genome Res 21:741–747

Fu Y, Ge Y, Sun Y, Liang J, Wan L, Wu X, Xu A (2015) IVT-SAPAS: low-input and rapid method for sequencing alternative polyadenylation sites. PLoS ONE 10:e0145477

Hilgers V, Perry MW, Hendrix D, Stark A, Levine M, Haley B (2011) Neural-specific elongation of 3′ UTRs during Drosophila development. Proc Natl Acad Sci USA 108:15864–15869

Hopper SA, White ME, Twiddy N (1992) An outbreak of blue-eared pig disease (porcine reproductive and respiratory syndrome) in four pig herds in Great Britain. Vet Rec 131:140–144

Hoque M, Ji Z, Zheng D, Luo W, Li W, You B, Park JY, Yehia G, Tian B (2013) Analysis of alternative cleavage and polyadenylation by 3′ region extraction and deep sequencing. Nat Methods 10:133–139

Ji Z, Lee JY, Pan Z, Jiang B, Tian B (2009) Progressive lengthening of 3′ untranslated regions of mRNAs by alternative polyadenylation during mouse embryonic development. Proc Natl Acad Sci USA 106:7028–7033

Ji L, Zhou X, Liang W, Liu J, Liu B (2017) Porcine interferon stimulated gene 12a restricts porcine reproductive and respiratory syndrome virus replication in MARC-145 cells. Int J Mol Sci 18:1613

Jia X, Yuan S, Wang Y, Fu Y, Ge Y, Ge Y, Lan X, Feng Y, Qiu F, Li P, Chen S, Xu A (2017) The role of alternative polyadenylation in the antiviral innate immune response. Nat Commun 8:14605

Kappes MA, Faaberg KS (2015) PRRSV structure, replication and recombination: origin of phenotype and genotype diversity. Virology 479–480:475–486

Ke W, Fang L, Jing H, Tao R, Wang T, Li Y, Long S, Wang D, Xiao S (2017) Cholesterol 25-hydroxylase inhibits porcine reproductive and respiratory syndrome virus replication through enzyme activity-dependent and -independent mechanisms. J Virol 91:e00827-17

Li Y, Wu Z, Liu K, Qi P, Xu J, Wei J, Li B, Shao D, Shi Y, Qiu Y, Ma Z (2017) Proteomic analysis of the secretome of porcine alveolar macrophages infected with porcine reproductive and respiratory syndrome virus. Proteomics. https://doi.org/10.1002/pmic.201700080

Ma Z, Yang L, Zhang YJ (2018) Porcine reproductive and respiratory syndrome virus: propagation and quantification. Curr Protoc Microbiol 48:15M.1.1–15M.1.14

Mayr C, Bartel DP (2009) Widespread shortening of 3′UTRs by alternative cleavage and polyadenylation activates oncogenes in cancer cells. Cell 138:673–684

Proll MJ, Neuhoff C, Schellander K, Uddin MJ, Cinar MU, Sahadevan S, Qu X, Islam MA, Poirier M, Muller MA, Drosten C, Tesfaye D, Tholen E, Grosse-Brinkhaus C (2017) Transcriptome profile of lung dendritic cells after in vitro porcine reproductive and respiratory syndrome virus (PRRSV) infection. PLoS ONE 12:e0187735

Proudfoot NJ (2011) Ending the message: poly(A) signals then and now. Genes Dev 25:1770–1782

Rossow KD, Collins JE, Goyal SM, Nelson EA, Christopher-Hennings J, Benfield DA (1995) Pathogenesis of porcine

reproductive and respiratory syndrome virus infection in gnotobiotic pigs. Vet Pathol 32:361–373

Sandberg R, Neilson JR, Sarma A, Sharp PA, Burge CB (2008) Proliferating cells express mRNAs with shortened 3′ untranslated regions and fewer microRNA target sites. Science 320:1643–1647

Schlackow M, Marguerat S, Proudfoot NJ, Bahler J, Erban R, Gullerova M (2013) Genome-wide analysis of poly(A) site selection in *Schizosaccharomyces pombe*. RNA 19:1617–1631

Shi Y (2012) Alternative polyadenylation: new insights from global analyses. RNA 18:2105–2117

Sun Y, Fu Y, Li Y, Xu A (2012) Genome-wide alternative polyadenylation in animals: insights from high-throughput technologies. J Mol Cell Biol 4:352–361

Takagaki Y, Seipelt RL, Peterson ML, Manley JL (1996) The polyadenylation factor CstF-64 regulates alternative processing of IgM heavy chain pre-mRNA during B cell differentiation. Cell 87:941–952

Tian B, Manley JL (2013) Alternative cleavage and polyadenylation: the long and short of it. Trends Biochem Sci 38:312–320

Tian B, Hu J, Zhang H, Lutz CS (2005) A large-scale analysis of mRNA polyadenylation of human and mouse genes. Nucleic Acids Res 33:201–212

Ulitsky I, Shkumatava A, Jan CH, Subtelny AO, Koppstein D, Bell GW, Sive H, Bartel DP (2012) Extensive alternative polyadenylation during zebrafish development. Genome Res 22:2054–2066

Zhao F, Fang L, Wang D, Song T, Wang T, Xin Y, Chen H, Xiao S (2016) SILAC-based quantitative proteomic analysis of secretome of Marc-145 cells infected with porcine reproductive and respiratory syndrome virus. Proteomics 16:2678–2687